Original Article
cnj.araku.ac.ir

Cite This: Colloid Nanosci. J. 3(1) (2025) 533-546 DOI: 10.61882/CNJ.3.1.533

Surface-Modified γ-Alumina Nanoparticles for Efficient Adsorption of some Cationic Dyes from Wastewater

Masoud Saadati [1]*, Salva Sadigzadeh [2]

[1] Department of Science, Farhangian University, Tehran, Iran
[2] Department of Chemistry, Faculty of Science, University of Maragheh, Maragheh, Iran

ARTICLE INFO

Article History:
Received May 16, 2025
Revised Jun 12, 2025
Accepted Jun 12, 2025
Published July 15, 2025

Corresponding Authors:
Masoud Saadati
Email:
m.saadati@cfu.ac.ir

ABSTRACT

This study explores the removal of cationic textile dyes using γ-alumina nanoparticles modified with an anionic surfactant. The nanoparticles were synthesized in the laboratory and subsequently modified with sodium dodecyl sulfate (SDS). These modified nanoparticles were utilized to eliminate two prevalent cationic dyes, basic yellow 40 and basic red 18, from aqueous solutions that emulate textile industrial effluents. Characterization analyses, including scanning electron microscopy (SEM), X-ray diffraction (XRD), and Fourier-transform infrared spectroscopy (FTIR), confirmed the successful synthesis and surface modification of the nanoalumina. To optimize the conditions for dye removal, a response surface methodology (RSM) was employed to evaluate the effects of contact time, dye concentration, adsorbent dosage, and solution pH at three levels each. Under optimized conditions, SDS-modified γ-alumina nanoparticles demonstrated a dye removal efficiency of over 94%. In tests with dye-spiked real samples, they maintained high adsorption efficiencies above 90%, much better than unmodified nanoparticles, which showed less than 60% efficiency. These results show that surfactant-modified nanoalumina is a strong and effective option for cleaning dye-contaminated wastewater.

KEYWORDS: *γ-alumina nanoparticles, Dye removal, Cationic textile dye, Textile effluent, Response Surface Methodology*

Introduction

The removal of textile dyes from water is a critical environmental and public health concern due to the extensive use of synthetic dyes in the textile industry. These dyes, often complex organic molecules, are discharged in significant quantities into water bodies, leading to severe water pollution. Their presence in aquatic environments not only imparts vivid coloration to water, which reduces light penetration and disrupts photosynthetic activity, but also introduces potentially toxic, carcinogenic, and mutagenic compounds into ecosystems [1,2].

Recent advancements in textile dye removal from wastewater have introduced innovative and efficient methods. These techniques aim to enhance dye degradation efficiency, minimize environmental impact, and promote sustainability. A novel approach involves using magnetic nanocomposites, such as iminodiacetic acid-functionalized graphene oxide combined with Fe_3O_4 (IDA-GO@Fe_3O_4). This composite effectively adsorbs both cationic and anionic dyes, like methylene blue and methyl orange. Its magnetic properties facilitate easy separation from treated water, and it demonstrates excellent recyclability over multiple cycles [3]. Laser-synthesized TiN nanoparticles have also emerged as efficient sorbents for dye removal. Their porous structure and electrostatic properties enable high adsorption capacities and offer a promising solution for environmental water cleaning [4]. Integrating

biopolymers like chitosan, cellulose, and alginate with advanced oxidation processes enhances dye degradation. These biopolymers serve as supports for catalysts, improving the efficiency of processes like photocatalysis and Fenton reactions, while being biodegradable and environmentally friendly [5]. Conducting polymers, notably polyaniline (PANI) and polypyrrole (PPy), have been utilized to create composites that effectively remove dyes from aqueous solutions. These materials function as adsorbents and photocatalysts, offering high efficiency in dye degradation [6]. Green photocatalysts synthesized from plant extracts or agricultural waste have shown promise in degrading various dye molecules under light irradiation. These eco-friendly catalysts generate reactive oxygen species that break down dyes, offering a sustainable approach to wastewater treatment [7]. Fungi-based remediation, or mycoremediation, as another approach employs fungal species to degrade dyes through enzymatic activity. This method is cost-effective and leverages natural biological processes for dye removal [8]. A novel magnetic nanocomposite composed of zeolite and cellulose nanocrystals (CNC) was developed for the adsorption removal of the cationic dyes' methylene blue and methyl violet 2B. The adsorption process was found to be spontaneous and exothermic, as demonstrated by thermodynamic analyses [9].

Recent advancements have highlighted the efficacy of gamma-phase nanoalumina (γ-Al_2O_3) in wastewater treatment, particularly for the removal of heavy metals and organic pollutants. Its high surface area, porosity, large number of active sites, availability and chemical stability make it a promising material for various treatment applications [10]. A study introduced a γ-Al_2O_3/carbon hollow nanosphere composite synthesized from orange peel waste. This composite demonstrated optimal removal of Ni^{2+} ions from wastewater, achieving high adsorption capacities and showcasing potential for reuse in forensic applications like blood fingerprint enhancement [11]. Wang et al. developed a magnetic composite catalyst comprising γ-Al_2O_3/TiO_2/γ-Fe_2O_3. This catalyst effectively degraded ibuprofen in wastewater through ozonation, with GC–MS analysis confirming the significant reduction of organic pollutants, including bisphenol A and sulfamethoxazole [12]. Research by Khatamian et al. focused on synthesizing nano γ-alumina and magnetite-alumina nanocomposites for nitrate adsorption. The proposed composite achieved up to 74% nitrate removal at 50 mg L^{-1} concentration, highlighting its potential in treating nitrate-contaminated water [13]. These studies underscore the versatility of γ-Al_2O_3-based materials in addressing diverse wastewater contaminants, offering sustainable and efficient treatment solutions.

In developing countries, the textile industry predominantly utilizes synthetic dyes such as azo, reactive, acidic, and cationic dyes due to their cost-effectiveness and diverse color options. However, the discharge of untreated dye-containing wastewater poses severe environmental hazards, contaminating aquatic ecosystems with toxic and persistent pollutants [14]. Studies highlight that conventional dyeing processes also entail high water and energy consumption. To mitigate these impacts, recent research focuses on eco-friendly alternatives, including natural dyes and advanced techniques like nanomaterial-assisted aimed at reducing water and chemical usage and improving sustainability in textile dyeing practices [15, 16].

The efficacy of gamma nanoalumina in treating wastewater contaminated with textile dyes has also been demonstrated in other studies. γ-Al_2O_3 nanoparticles were used to adsorb Reactive Red 141 dye from aqueous solutions. The study analyzed process modeling, kinetics, and isotherms to understand the adsorption mechanism [17]. Furthermore, alumina nanoparticles have been utilized for the removal of Zn (II) and Color Black G dye from wastewater, thereby demonstrating effective adsorption capabilities [18]. The surface of alumina nanoparticles can be modified to create a new and efficient adsorbent that can remove pollutants, including dyes, from aqueous solutions with high efficiency. Polycation-modified nano alumina particles were utilized for the adsorptive removal of the azo dye New Coccine [19]. Nano γ-Al_2O_3 modified with surfactants demonstrated enhanced adsorption of cationic dyes, such as rhodamine B and methylene blue from industrial wastewater [20, 21], basic yellow 28 and basic brown 41 dyes from textile effluents [22], and acid orange G azo from aqueous solutions [23] achieving high removal efficiencies and adsorption capacities. The removal of rhodamine B using SDS-modified α-Al_2O_3 was also investigated, and the results demonstrated significantly higher efficiency compared to raw α-Al_2O_3 [24]. We reported here an alumina nanoparticle-based method to remove two

common dyes used in the Iranian textile industry from effluents. The nanoparticles were synthesized in the laboratory, characterized, modified with an anionic surfactant, and successfully performed to remove two cationic dyes, basic red 18 (BR18) and basic yellow 40 (BY40), from aqueous solutions of textile industrial effluents. To optimize the parameters affecting dye removal the response surface method (RSM) was used.

Materials and methods

Reagents and apparatus

All reagents used in these experiments, except those indicated, were of analytical grade purchased from Merck (Darmstadt, Germany). Textile dyes basic yellow 28 (BY28), basic blue 41 (BB41), basic brown 1 (BB1), basic red 46 (BR46), acidic yellow 17 (AY17), acidic blue 7 (AB7), BR18, and BY40, were obtained from Alvan Sabet Co. (Hamedan, Iran) and Alan Chemical Industries Ltd (China). The absorption spectra of the dye solutions were recorded and the light absorption was measured using a UV-Vis spectrophotometer (SPECOL 2000, Analytik Jena, Germany). The structure of the synthesized nanoparticle was determined using an FT-IR spectrometer (Tensor 27, USA), an X-ray diffractometer (PW 1730, Netherlands), and a scanning electron microscope (FE-SEM, TESCAN MIRA3, Czech Republic). An electric oven manufactured by Fan Azma Gostar Co. (Iran) was also utilized in this study.

Synthesis of gamma alumina nanoparticles

Synthesis of nano gamma alumina was conducted within the laboratory setting, employing a sol-gel methodology [22]. Initially, 22.5 g of sodium nitrate were accurately weighed and placed in a beaker. Subsequently, 10 mL of distilled water were added and mixed thoroughly using a magnetic stirrer until a uniform solution was achieved. The solution was then filtered through filter paper and a funnel, resulting in the creation of solution number one. In another beaker, 0.11 g of cetyltrimethylammonium bromide (CTMAB) were combined with 5 mL of distilled water, stirred for 40 min, and stored as solution number two. For solution number three, 2.5 g of ammonium bicarbonate were added to a 50 mL beaker, followed by the addition of 10 mL of distilled water, and the mixture was thoroughly blended using a magnetic stirrer. Subsequently, solution number two was slowly added to solution number one using a graduated burette over five hours. Following this, solution number three was gradually introduced over a 24-hour period. The resulting mixture was continuously stirred for an hour to ensure homogeneity, before being left at room temperature for 72 hours to allow gel formation, covered with parafilm. The gel was then transferred to an oven and heated at a temperature range of 80 °C for 10 hours to eliminate all water content. Following a cooling period, the solid material was separated from the container. It was then stored for a duration of one day. Thereafter, the collected material underwent calcination in an electric furnace at a temperature of 500 °C for a period of five hours. This process was undertaken to transform the alumina into a porous texture.

Surface modification of alumina nanoparticles

The surface of the synthesized gamma nano alumina was modified using the anionic surfactant sodium dodecyl sulfate (SDS) for its application in the dye removal process. A 2 g sample of nano alumina was mixed with 20 mL of a solution containing 0.4 g of SDS, followed by the addition of 0.05 g of sodium chloride. The pH of the solution was adjusted to 4±0.2. After stirring for 7 hours and allowing the solid particles to settle, the supernatant liquid was discarded. The modified nano-gamma alumina was then washed five times with distilled water. The prepared adsorbent was dried in an oven at 60°C for 24 hours. Once fully dried, the nanoparticles were transferred to a sealed container for storage.

Optimization and modeling of dye removal process by response surface method

To optimize the removal of cationic dyes using modified nanoparticles and achieve maximal dye removal, the response surface method and Box–Behnken design techniques were employed. Based on prior research, four major factors were determined to significantly influence the process: pH, contact time (min), adsorbent dosage (amount of adsorbent for a specific volume of dye solution), and dye concentration (mg L^{-1}) [22]. These factors were explored at three levels: 15, 37.5, and 60 min for stirring time, 5, 30, and 55 mg L^{-1} for dye concentration, 2, 4, and 6 g L^{-1} for adsorbent dose, and pH levels of 2, 4, and 6. The experiments were designed and analyzed using Minitab21 software in accordance with the Box–Behnken designs, which

Table 1. The 27 runs of RSM using Box–Behnken experimental designs

RunOrder	pH	Time	Adsorbent	Dye Con
1	4	15.0	4	5
2	4	37.5	4	30
3	6	37.5	6	30
4	6	15.0	4	30
5	2	60.0	4	30
6	4	37.5	4	30
7	4	60.0	4	55
8	4	37.5	6	55
9	4	15.0	2	30
10	2	37.5	4	55
11	4	15.0	6	30
12	4	37.5	2	55
13	4	37.5	6	5
14	2	37.5	6	30
15	2	37.5	2	30
16	6	37.5	4	55
17	2	37.5	4	5
18	4	37.5	2	5
19	6	60.0	4	30
20	4	15.0	4	55
21	2	15.0	4	30
22	4	60.0	6	30
23	6	37.5	2	30
24	6	37.5	4	5
25	4	60.0	4	5
26	4	37.5	4	30
27	4	60.0	2	30

necessitated 27 experiments conducted across the three levels of the four variables. Detailed results are presented in Table 1.

Performing optimization experiments

In order to conduct the optimization experiments, solutions containing two types of dyes, BR18 and BY40 were prepared at three different concentrations (5, 30, and 55 mg L^{-1}). 10 mL of each dye solution was transferred into individual beakers, followed by the addition of the required quantity of nano adsorbent based on the recommended weight. The pH of each solution was then adjusted using a prepared buffer and monitored using a pH meter. The samples were stirred on a magnetic stirrer until the designated time to facilitate the absorption of the dye by the nano adsorbent. Subsequently, the supernatant solution was separated from the nanoparticles, and its absorbance was measured using a UV-Vis spectrophotometer at the maximum wavelength. The UV-Vis colorimetric spectrum of the dyes confirmed that the maximum wavelengths for absorbance measurements were 528 nm for BR18 and 435 nm for BY40. The percentage of dye removal was determined by comparing the absorption levels before and after the addition of nanoparticles in each of the 27 experiments.

Result and discussion

Identification of gamma alumina nanoparticles

X-ray diffraction (XRD) analysis was utilized to investigate and validate the synthesis of gamma nanoalumina particles. According to the Scherrer equation, the peak widths at half maximum intensity (FWHM) increase with decreasing particle size of the material. The XRD pattern acquired for the synthesized sample (Figure 1) displays the presence of a distorted and rhombic crystalline structure measuring approximately 25 nanometers, with a 2θ diffraction peak at around 66.70, confirming the successful synthesis of gamma nanoalumina.

As demonstrated in Figure 2, the FTIR spectra of unmodified and modified nano gamma alumina, as well as SDS, are presented for comparison. The observed peaks for unmodified nanoparticles at approximately 592 cm-1 are attributed to the bending vibration of the Al-O bond, the peak at around 783 cm-1 is associated with the stretching vibration of the Al-O bond, and the observed peak at 1428 cm-1 corresponds to the bending vibration of the -CH3 group. The observed peaks at 1527 and 1637 cm-1 are attributed to the presence of carboxylic groups, while the broad peak at 3441 cm-1 is associated with the stretching vibration of the O-H bond in the observed H2O molecules [25].

In the FTIR spectra associated with SDS, the peaks at 590, 632, and 834 cm^{-1} correspond to the symmetric bending vibration of the C-H bond in the -CH_2 group [26]. The observed peak at approximately 1087 cm^{-1} is attributed to the stretching vibration of the C-C bond, while the peaks at around 1220 and 1222 cm^{-1} are linked to the stretching vibration of the S-O bond. The broad peak observed at approximately 3467 cm^{-1} is indicative of the stretching vibration of the H-OH bond [27]. The corresponding peaks of unmodified nanoparticles and SDS in comparison to modified nanoparticles are observed with lower intensity, which confirms the interaction of surface modification of gamma alumina nanoparticle with SDS. For instance, the observation of a peak at approximately 1250 cm^{-1} indicates the stretching vibration of the S=O bond. This peak is not present in the spectrum of unmodified alumina nanoparticles; however, it is evident in the spectrums of SDS and modified nanoparticles. This finding suggests that SDS is absorbed on the surface of alumina nanoparticles from the negative end. Furthermore, the presence of the peaks at 2852, 2920, and 2958 cm^{-1} in the spectrum of modified nano alumina particles indicates the presence of SDS on the surface of modified alumina nanoparticle. The adsorption of the anionic SDS on gamma nano alumina is distinct from its adsorption on activated Al_2O_3 grains, where electrostatic attraction is the predominant driving force. In this case, the process of SDS adsorption

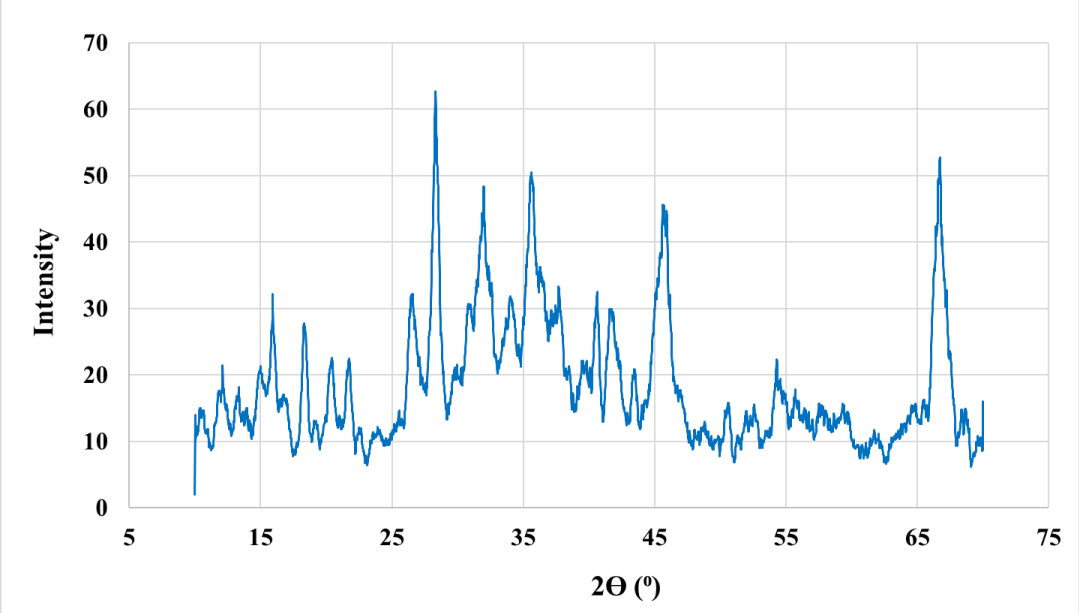

Fig. 1. XRD spectrum of modified nano gamma alumina

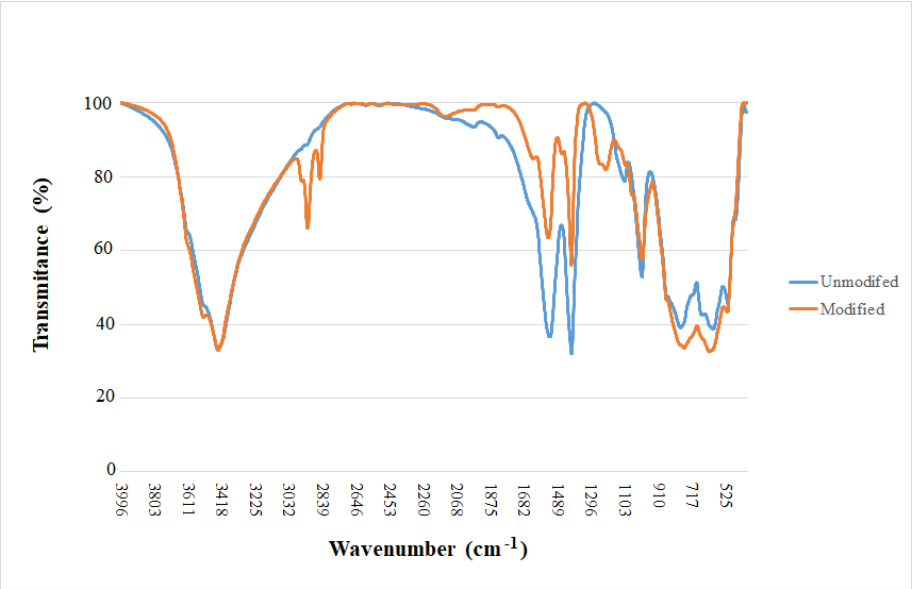

Fig. 2. FTIR of modified and unmodified gamma alumina nanoparticles

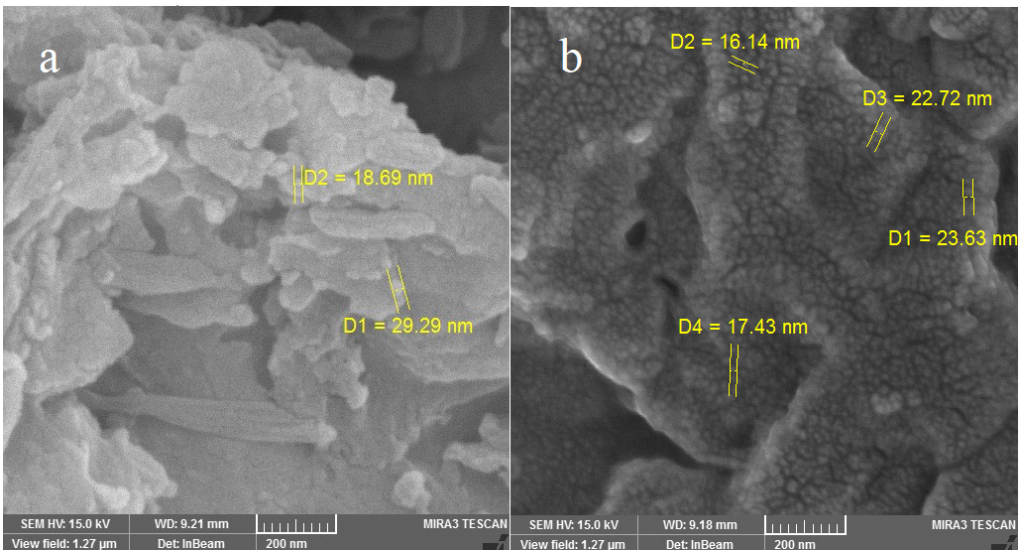

Fig. 3. SEM for **(a)** Modified and **(b)** Unmodified nano gamma alumina sample

on nano gamma alumina is governed by a dual mechanism, namely electrostatic and hydrophobic interactions [20].

The SEM images (Figures 3a and 3b) show that the synthesized alumina nanoparticles are nanoscale in size, around 25 nm as confirmed by XRD analysis. The unmodified nanoparticles maintain structural integrity, while those modified with SDS surfactant exhibit a porous surface. The modification was precise and followed specified parameters. Importantly, the SDS-modified nanoparticles enhance dye removal efficiency from textile effluents compared to unmodified ones.

Investigating the factors affecting the amount of dye removal using the RSM

As illustrated in Figure 4, the three-dimensional diagram was obtained from the Minitab software to determine the simultaneous influence of two different factors at three distinct levels for the removal percentage of the cationic BY40 dye.

Figure 4a illustrates the response curve to the

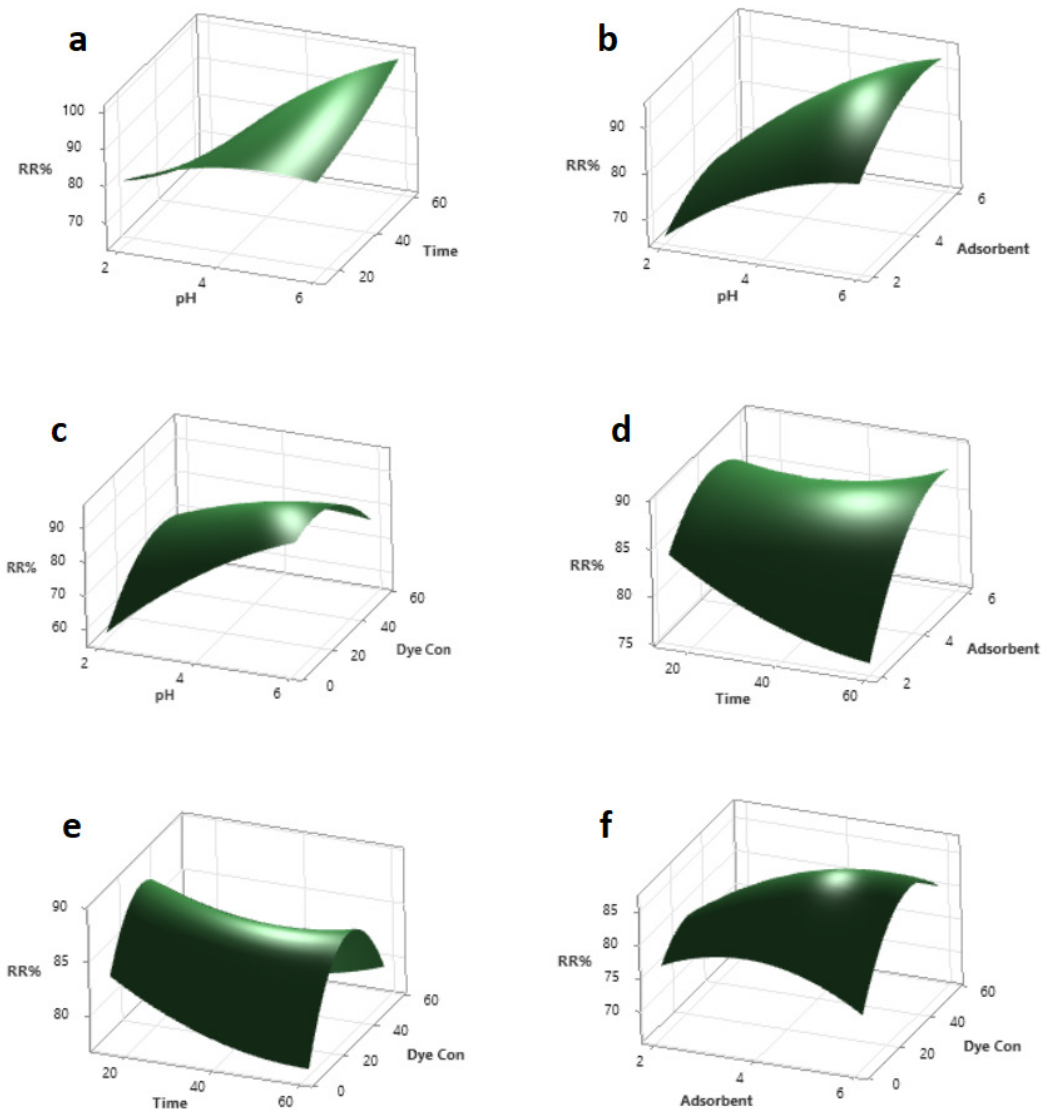

Fig. 4. Three dimensional graphs of response surface graphs related to the removal of BY40, as a function of **(a)** dye concentration and stirring time, **(b)** amount of adsorbent and time, **(c)** amount of adsorbent and dye concentration, **(d)** pH and time, **(e)** pH and dye concentration, and **(f)** pH and amount of adsorbent.

effect of two factors, pH and stirring time, on the rate of dye removal in conditions where the other two factors, namely the amount of absorbent and the dye concentration, are at the middle level, 4 g L^{-1} and 30 mg L^{-1}, respectively. As can be seen, the dye removal increases significantly with a pH value of 0 to 8, and the most suitable pH for this process is 6. Conversely, at higher pH values, the percentage of dye removed decreases, as does the amount of dye removal achieved at the shortest stirring time. This value demonstrates a negative correlation with increasing stirring time at a gentle slope. According to Figure 4a, the optimal conditions for BY40 dye removal are as follows: a pH of approximately 6 and a stirring time of approximately 15 min.

Figure 4b shows the response surface curve of the effect of pH and adsorbent dosage while the other factors are in mediate level. As mentioned earlier, the pH level has a big impact on how well the dye removal process works. You can see this

effect in the 3D response surface diagram. If the pH level goes from 1 to 8, the percentage of dye removal goes up a lot.

However, the impact of increasing the amount of dye removed was almost nonexistent as the amount of absorbent increased from 2 to 6 g L^{-1}. This suggests that the amount of dye removed is not very affected by the amount of absorbent. Figure 4b shows that maximum dye removal occurred at a pH of around 6, with efficiency decreasing at higher pH levels. Optimal adsorbent dosage was also around 6, but its effectiveness declined over time.

Figure 4c illustrates the response surface curve, which demonstrates the effect of pH and dye concentration at the central levels of stirring time (37.5 min) and adsorbent dose (0.04 g/10 ml) and ambient temperature on the dye removal rate. The highest dye removal rate occurs at low dye concentrations and a pH of around 6. As dye concentration increases, removal efficiency drops significantly, while higher pH levels improve removal up to pH 6, after which efficiency declines. Figure 4c illustrates these optimal conditions.

Figure 4d shows the response surface curve of how stirring time and adsorbent dose at central levels of dye concentration (30 mg L^{-1}) and pH (6) affect the rate of BY40 dye removal. According to the figure, as the adsorbent dose increases, the percentage of dye removal also increases, but this increase occurs with a gentle slope. It is clear from the obtained diagram that the highest dye removal occurs with a stirring time of about 15 min and an adsorbent dosage of 0.06 g/10 ml, with optimal efficiency achieved between 15 to 20 min of stirring.

As illustrated in figure 4e, the response surface curve demonstrates the impact of stirring time and dye concentration on BY40 dye removal. According to the figure, the rate of dye removal increases with decreasing concentration and with increasing stirring time. Consequently, these alterations occur with a gentle slope. Figure 4f illustrates the effect of dye concentration and adsorbent dosage on BY40 removal. The percentage of dye removal also increases with increasing adsorbent dosage and with decreasing dye concentration. Consequently, the figure indicates that the maximum dye removal was achieved at an adsorbent dosage of 6 g L^{-1} and a dye concentration of approximately 30 mg L^{-1}. Figure 5a presents the response surface curve of the effect of pH and stirring time at the middle levels of two other factors, the amount of adsorbent (4 g L^{-1}) and the concentration of dye (30 mg L^{-1}), in the BR18 dye removal process. As the pH level rises, the efficiency of dye removal exhibits a marked increase. According to observations, the most suitable pH for this process is 6, as above this value, the percentage of dye removal decreases. The highest dye removal occurred at the shortest stirring time, and as stirring time increased, dye removal gradually decreased. Consequently, the maximum dye removal is attained at a pH of approximately 6 and a stirring duration of about 15 min.

Figure 5b illustrates the response surface curve of the effect of pH and adsorbent dosage on BR18 dye removal. The 3D response surface diagram illustrates the substantial impact of pH on the efficiency of dye removal process. An increase in pH from 1 to 6 has been shown to significantly enhance dye removal, while an increase in the absorbent amount from 2 to 6 g L^{-1} only yields a modest improvement in dye removal. This increment in absorbent concentration exhibited a negligible effect on the percentage of dye removal. The maximum dye removal was observed at approximately pH 5, after which it exhibited a decline at higher pH values. The highest observed dye removal was attained at an adsorbent dosage of approximately 5, with only a marginal increase in removal observed as dosage varied.

Figure 5c illustrates the response surface curve, demonstrating the impact of pH and dye concentration on dye removal. As demonstrated in Figure, the efficacy of dye removal is maximized at elevated pH levels and reduced dye concentrations. As the dye concentration increases, the percentage of dye removal experiences a notable decrease, exhibiting minimal impact on the overall removal efficiency. The rate of dye removal remained constant between 5 and 30 mg L^{-1} dye concentrations, then gradually decreased. The highest removal rate occurred around pH 6, after which it declined. This suggests that optimal dye removal at low dye concentrations and a pH near 6 is possible.

As illustrated in Figure 5d, the response surface curve demonstrates the impact of stirring time and adsorbent dosage on the BR18 dye removal rate. This rate was measured at a middle level of two other factors: a dye concentration of 30 mg L^{-1} and a pH of 6, as well as ambient temperature. Increasing adsorbent dosage slightly improves dye removal, with the highest removal occurring at about 15 min

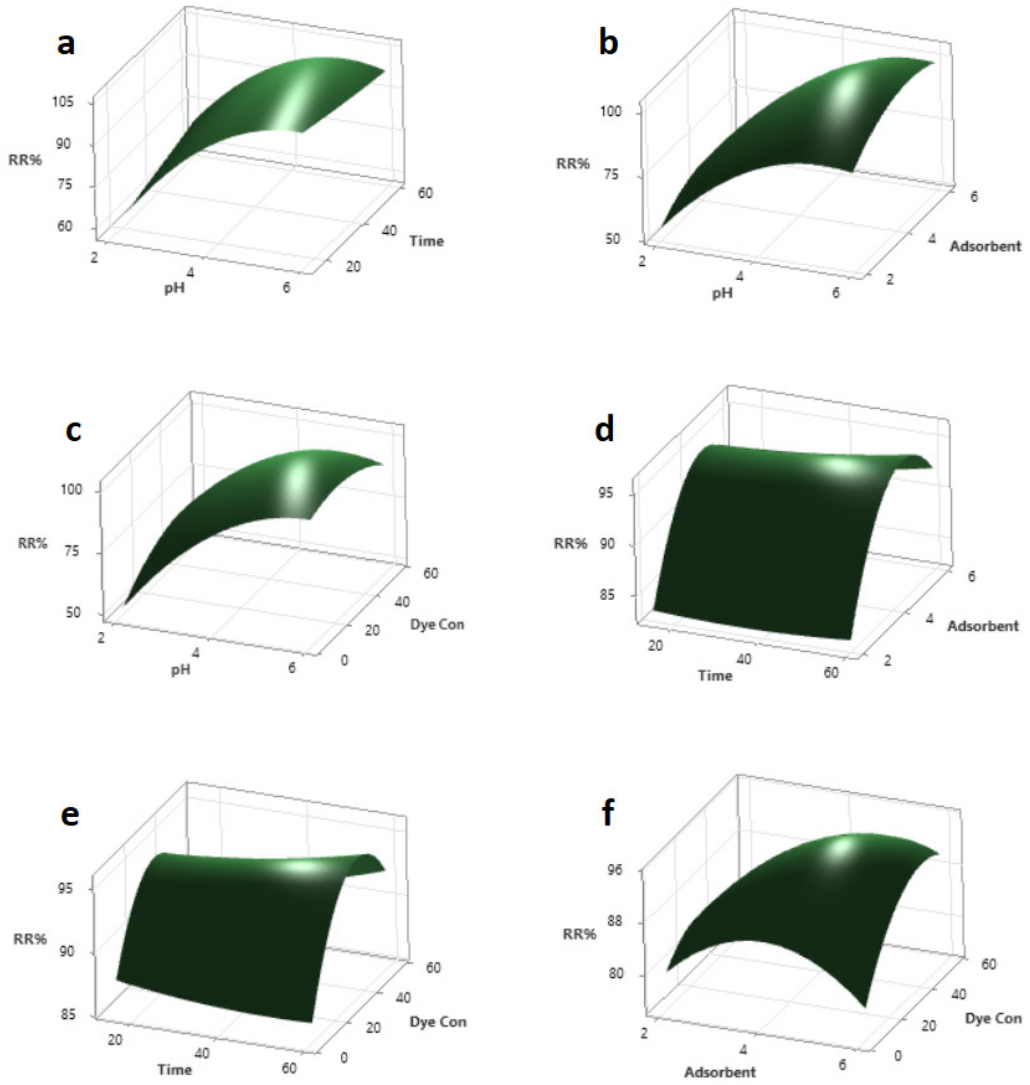

Fig. 5. Three dimensional graphs of response surface graphs related to the removal of BR18, as a function of **(a)** dye concentration and stirring time, **(b)** amount of adsorbent and dye concentration, **(c)** pH and dye concentration, **(d)** pH and time, **(e)** amount of adsorbent and time, and **(f)** pH and amount of adsorbent.

of stirring and 5 g L^{-1} adsorbent dosage.

Figure 5e presents the response surface curve, which illustrates the effect of stirring time and dye concentration on dye removal. The figure was developed under fixed conditions of pH 4, an adsorbent dosage of 4 g L^{-1}, and ambient temperature. The figure indicates that dye removal rate increases as dye concentration decreases, and the dye removal percentage improves with longer stirring times.

Figure 5f presents the response surface curve, which illustrates the effect of dye concentration and adsorbent dosage. These variables were measured at a constant middle level of pH (4) and stirring time (37.5 min). The figure shows that dye removal increases with higher adsorbent dosage and lower dye concentration, with maximum BR18 dye removal at 6 g L^{-1} adsorbent and around 30 mg L^{-1} dye concentration.

The ANOVA tables analysis

In order to assess the adequacy of a model, it

Table 2. Adsorption capacity and removal efficiency of surfactant-modified nano-Al_2O_2 for various dyes

Adsorbent	Studied dyes	Adsorption capacity (mg g^{-1})	Efficiency (%)	References
Polycation-Modified-α-Al_2O_3	New Coccine	13.5	<53	[19]
SDS modified-γ-Al_2O_3	Rhodamine B	165	>86	[20]
SDS modified-γ-$Al_{2O}3$	BR46 and BB1	10	>93	[22]
Polycation-Modified-α-Al_2O_3	Acid Orange G	9.1	90.1	[23]
SDS modified-α-Al_2O_3	Rhodamine B	52	>98	[24]
SDS modified-γ-Al_2O_3	BY40 and BR18	10.6	>94	Present work

is necessary to examine the p-values for both the model and the lack of fit in the ANOVA table. A model is deemed statistically significant if its p-value is less than 0.05, indicating a confidence level greater than 95%, thereby substantiating the reliability of the obtained results. In this study, the p-value for the model corresponding to the BY40 dye is 0.009, and for the BR18 dye, it is 0.001. These values correspond to confidence levels of 80.79% for BY40 and 78.35% for BR18, respectively. In the event of lack of fit—that is, the model's inability to adequately represent the experimental data—the p-value should exceed 0.05 to indicate that the lack of fit is not statistically significant. For BY40 and BR18 dyes, the lack of fit p-values is 0.156 and 0.053, respectively, both of which fall within the acceptable range. These findings indicate that the models employed are both appropriate and reliable. Additionally, the analysis suggests that the pH is the most significant parameter affecting dye removal, in comparison to the other variables.

According to the optimized conditions for BY40 dye, the following parameters were introduced by the program: stirring time of 40 min, pH=6, adsorbent dosage of 6 g L^{-1}, and dye concentration of 15 mg L^{-1}. The program's estimation for the dye removal percentage in these conditions was 98.77%. The dye removal test was conducted in these conditions, yielding a percentage of 96.50%. According to the optimized conditions for BR18 dye, the following parameters were introduced by the program: stirring time of 15 min, pH = 6, adsorbent dose of 4.5 g L^{-1}, and dye concentration of 10 mg L^{-1}. The percentage of dye removal predicted by the program was 97.86%. The experiment yielded an observed percentage of dye removal of 95.12%, which differs from the program's prediction. This discrepancy can be attributed to the fact that the dye removal process was conducted under conditions that were not perfectly optimal.

To the best of our knowledge, the removal of BY40 and BR18 dyes has not been investigated previously. Nevertheless, the adsorption capacity and removal efficiency in this work were compared with other methods based on surfactant-modified nano-alumina (Table 2). The results demonstrate that the proposed method achieves competitive adsorption capacity and acceptable removal efficiency compared to existing approaches.

Although the present work and our previous study [22] share a similar method for synthesizing nano-alumina and some methodological steps show unavoidable similarities, the obtained results differ significantly. In these works, the removal of different dyes was investigated for the first time using SDS modified γ-Al_2O_3. The optimal conditions and analytical performance metrics differ between the two studies. This demonstrates that the findings from the previous work cannot be generalized to the current one, necessitating independent research. This observation is further supported by comparison with other studies in Table 2, which utilized the same adsorbent for the removal of different dyes.

Evaluation of optimal conditions in the real sample

The efficacy of modified nanoparticles in the removal of dyes from actual samples was assessed by quantifying the percentage of dye eliminated

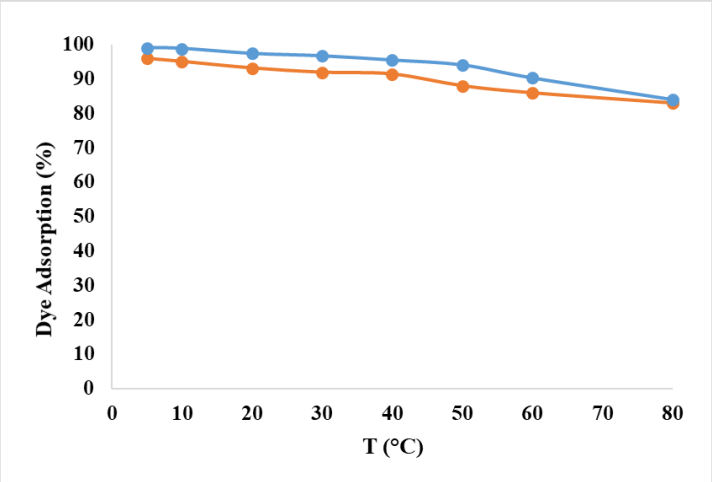

Fig.6. Adsorption of BY40 (yellow) and BR18 (blue) dyes at different temperatures

Table 3. Tolerable concentration ratios for determination of 5 mg L^{-1} of each dye with the proposed method (relative error ± 5%).

Interfering species	BY40	BR18
basic brown 1	4	6
basic red 46	5	1
Basic yellow 28	1	5
Basic blue 41	6	6
Basic yellow 40	-	5
Basic red 18	5	-
acid yellow 17	10	10
acid blue 7	10	10
Ca^{2+}	500	500
K^{+}	1000	500
Fe^{2+}	1000	400
Na^{+}	250	1000

under optimal conditions. The authentic sample was meticulously prepared in the laboratory using materials and components that are representative of those in the original sample. In the context of the real sample, the dye removal efficiency was found to be 92.03% for BY40 and 94.56% for BR18, under optimal conditions. The chemical composition of the authentic sample encompasses nitrate and nitrite, iron and manganese, suspended solids, sulfate, phosphate, chloride, fluoride, calcium, and sodium, along with other trace elements. The percentage of these elements is consistent with their amount in municipal water.

Analysis of the temperature effect on dye removal

In order to ascertain the effect of temperature on the dye removal, a series of experiments were conducted at temperatures ranging from 5 to 80°C. These temperatures corresponded to the optimal dye removal conditions, and the percentage of dye removal was measured at each temperature. The results obtained (Figure 6) indicate that the optimal temperature is 20°C. This temperature is advantageous due to its prevalence,

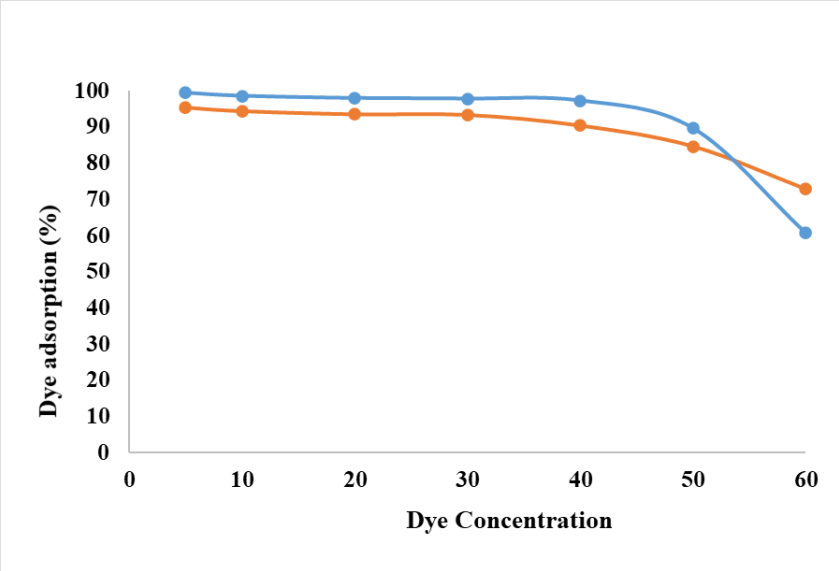

Fig. 7 The adsorption capacity of BY40 (yellow) and BR18 (blue) dyes at varying adsorbent dosages under optimal conditions

ease of provision, and minimal time and energy requirements.

Evaluation of optimal conditions using unmodified nanoparticles

To investigate the effect of surface modification on dye removal efficiency, unmodified nanoparticles were used under optimal conditions. The dye removal percentages obtained for BY40 and BR18 were 55.21% and 59.13%, respectively. These results, when compared with those obtained for the modified nanoparticles, clearly demonstrate the importance of surface modification and its significant impact on the efficiency of nanoparticles in dye removal.

Interference study

To study the effectiveness of the proposed method for removing BY28 and BB41 dyes in the presence of other dyes and ions, an interference study was performed by analyzing solutions containing the primary dye and interfering dyes or ions. The results, with a maximum tolerable error of 5%, are presented in Table 3.

The adsorbent's maximum dye removal capacity

To study the dye absorption capacity of a specific amount of modified nanoalumina adsorbent and its capacity to remove the studied dyes, an experiment was conducted under optimal conditions for each dye by changing the analyte concentration. For each study, 150 mg of the adsorbent were added to 50 mL of the analyte, which contained variable amounts ranging from 5 to 60 mg L^{-1} - the range of dye concentrations present in textile wastewater. The amount of dye removal or absorption by the adsorbent was calculated under optimal conditions. The results are presented in Figure 7.

Conclusion

The synthesis and modification of gamma alumina nanoparticles with sodium dodecyl sulfate (SDS) surfactant was conducted. These nanoparticles were then employed as a novel and efficient adsorbent for the removal of cationic dyes BY40 and BR18 from aqueous solutions of industrial wastewater. The efficacy of the adsorbent was confirmed by XRD, FTIR, and SEM analyses. The surface modification of the nanoparticles was precisely performed, resulting in the development of porosity within their structural framework. This increased porosity was demonstrated to improve the efficiency of dye removal.

The investigation of additional textile dyes, including acid dyes alongside cationic dyes, as well as the assessment of dye removal rates in their presence, demonstrates the selective efficacy of the modified nanoparticles toward cationic dye removal. The findings revealed that the modified nanoparticles exhibited a substantially superior dye-removal capacity when compared to their unmodified counterparts. Moreover, the evaluation of potential interference from other dyes and

various ions during the removal of BY40 and BR18 dyes supports and validates this selective removal capability.

Acknowledgements

We would like to express our sincere gratitude to Farhangian University for their invaluable support and resources during this project.

Declarations

Competing interest The authors declare that they have no competing financial interests or personal relationships that could have influenced the work reported in this paper.

Ethical approval This article does not require ethical approval.

Consent to participate The authors of the study attest that all of the data presented are real experimental results.

Consent to publish The study does not involve any human participants, human data, or human tissues.

Funding Not applicable.

References

[1] T. Islam, M.R. Repon, T. Islam, Z. Sarwar, M.M. Rahman, Impact of textile dyes on health and ecosystem: a review of structure, causes, and potential solutions Environ Sci Pollut Res. 30 (2023) 9207–9242. https://doi.org/10.1007/s11356-022-24398-3

[2] A.P. Periyasamy, Recent Advances in the Remediation of Textile-Dye-Containing Wastewater: Prioritizing Human Health and Sustainable Wastewater Treatment, Sustainability, 16(2) (2024) 495. https://doi.org/10.3390/su16020495

[3] A. Abdolmaleki, Z. Mohamadi, Z. Bazyar, A simple, efficient, and rapid method for dye removal from wastewater using an IDA-GO@Fe3O4 magnetic nanocomposite, RSC Adv. 14 (2024) 27843–27851. https://doi.org/10.1039/D4RA04555F

[4] A.V. Syuy, I.V. Martynov, I.A. Zavidovskiy, D.V. Dyubo, Q. Sun, X. Yang, G.V. Tikhonowski, D.I. Tselikov, M.S. Savinov, I.V. Sozaev, A.A. Popov, S.M. Klimentov, G.I. Tselikov, V.S. Volkov, S.M. Novikov, A.V. Arsenin, X. Zhao, A.V. Kabashin, Laser-synthesized TiN-based nanoparticles as novel efficient electrostatic nanosorbent for environmental water cleaning, Physica Scripta, 99 (2024) 115914. https://doi.org/10.1088/1402-4896/ad7cda

[5] D. Peramune, D.C. Manatunga, R.S. Dassanayake, V. Premalal, R.N. Liyanage, C. Gunathilake, N. Abidi, Recent advances in biopolymer-based advanced oxidation processes for dye removal applications: A review, Environ Res. 215 (2022) 114242. https://doi.org/10.1016/j.envres.2022.114242

[6] J. Stejskal, Recent Advances in the Removal of Organic Dyes from Aqueous Media with Conducting Polymers, Polyaniline and Polypyrrole, and Their Composites, Polymers, 14 (2022) 4243. https://doi.org/10.3390/polym14194243

[7] M. Kadhom, N. Albayati, H. Alalwan, M. Al-Furaiji, Removal of dyes by agricultural waste, Sustain. Chem. Pharm. 16 (2020) 100259. https://doi.org/10.1016/j.scp.2020.100259

[8] S.K. Sen, S. Raut, S. Raut, Mycoremediation of anthraquinone dyes from textile industries: a mini-review, BioTechnologia, 104 (2023) 85–91. https://doi.org/10.5114/bta.2023.125088

[9] S. Fındık, Removal of Cationic Dyes Methyl Violet 2B and Methylene Blue Using a Magnetic Zeolite-Cellulose Nanocrystal Nanocomposite: A Study on Single and Binary Dye Systems, Chem. Afr. (2025). https://doi.org/10.1007/s42250-025-01284-2

[10] R. Mahesh, K. Vora, M. Hanumanthaiah, A. Shroff, P. Kulkarni, S. Makuteswaran, S. Ramdas, H.L. Ramachandraiah, A.V. Raghu, Removal of pollutants from wastewater using alumina based nanomaterials: A review, Korean J. Chem. Eng. 40 (2023) 2035–2045. https://doi.org/10.1007/s11814-023-1419-x

[11] Y.B. Nthwane, B.G. Fouda-Mbanga, M. Thwala, K. Pillay, Novel synthesis of γ-Al2O3/carbon hollow nanosphere nanocomposite for the optimal removal of Ni2+ ions from wastewater and reuse in blood fingerprint enhancement, J. Iran. Chem. Soc. 21 (2024) 101–115. https://doi.org/10.1007/s13738-023-02909-4

[12] C. Wang, G. Zhou, Y. Xu, P. Yu, The Effect of Magnetic Composites (γ-Al2O3/TiO2/γ-Fe2O3) as Ozone Catalysts in Wastewater Treatment, Materials, 15(23) (2022) 8459. https://doi.org/10.3390/ma15238459

[13] M. Khatamian, S.K. Derakhshan, S.H. Nami, S. Fazli-Shokouhi, Nitrate removal study of synthesized nano γ-alumina and magnetite-alumina nanocomposite adsorbents prepared by various methods and precursors, Sci. Rep. 14 (2024) 7673. https://doi.org/10.1038/s41598-024-58459-z

[14] F. Uddin, Environmental hazard in textile dyeing wastewater from local textile industry, Cellulose, 28 (2021) 10715–10739. https://doi.org/10.1007/s10570-021-04228-4

[15] S.M. Sajjadi, G. Hossinzadeh, Textile dyes removing from the wastewater by green synthesized Cu-doped ZnO photocatalysts under the simulated sunlight illumination, Ceram. Int. 50 (2024) 36271–36285. https://doi.org/10.1016/j.ceramint.2024.07.011

[16] H. Pouresmaeil, G.R. Nabi Bidhendi, The use of Fe3O4/MnO2-Ag nano-photocatalyst to remove dyes from real wastewater samples under visible light, Int. J. Environ. Sci. Technol. 21 (2024) 10103–10114. https://doi.org/10.1007/s13762-024-05762-x

[17] Z. Bonyadi, Z. Fouladi, A. Robatjazi, M. Zahmatkesh Anbarani, Reactive red-141 removal from synthetic solutions by γ-Al2O3 nanoparticles: process modeling, kinetic, and isotherm studies, Appl. Water Sci. 13 (2023) 52. https://doi.org/10.1007/s13201-022-01854-6

[18] R.J. Bhargavi, U. Maheshwari, S. Gupta, Synthesis and use of alumina nanoparticles as an adsorbent for the removal of Zn (II) and CBG dye from wastewater, Int. J. Ind. Chem. 6 (2015) 31–41. https://doi.org/10.1007/s40090-014-0029-1

[19] T.H.Y. Doan, H.A. Pham, N.H. Nguyen, T.D. Le, T.B. Nguyen, T.S. Le, Adsorptive Removal of Azo Dye New Coccine Using High-Performance Adsorbent-Based Polycation-Modified Nano-Alpha Alumina Particles, J. Anal. Methods Chem. 2022 (2022) 9425334. https://doi.org/10.1155/2022/9425334

[20] T.P. Chu, N.T. Nguyen, T.L. Vu, T.H. Dao, L.C. Dinh, H.L. Nguyen, T.H. Hoang, T.S. Le, T.D. Pham, Synthesis, Characterization, and Modification of Alumina Nanoparticles for Cationic Dye Removal, Materials, 2019. https://doi.org/10.3390/ma12030450

[21] S. Ali, Y. Abbas, Z. Zuhra, I.S. Butler, Synthesis of γ-alumina (Al2O3) nanoparticles and their potential for use as an adsorbent in the removal of methylene blue dye from industrial wastewater, Nanoscale Adv. 1 (2019) 213–218. https://doi.org/10.1039/C8NA00014J

[22] M. Saadati, M. Iranifam, S.I. Mosavi, Removal of some textile cationic dyes from industrial wastewater using modi-

fied gamma alumina nanoparticles, J. Appl. Res. Chem. 17 (2024) 60–75. . http://sanad.iau.ir/en/Article/1044851

[23] T.H. Yen Doan, L. Van Dang, T.T. Trang Truong, T.N. Vu, T.S. Le, T.M. Thu Nguyen, M.N. Nguyen, T.T. Pham, S.-i. Yusa, T.D. Pham, Removal of Acid Orange G Azo Dye by Polycation-Modified Alpha Alumina Nanoparticles, Chem. Asian J. 18 (2023) e202300404. https://doi.org/10.1002/asia.202300404

[24] T.H. Yen Doan, T.P. Minh Chu, T.D. Dinh, T.H. Nguyen, T.C. Tu Vo, N.M. Nguyen, B.H. Nguyen, T.A. Nguyen, T.D. Pham, Adsorptive Removal of Rhodamine B Using Novel Adsorbent-Based Surfactant-Modified Alpha Alumina Nanoparticles, Journal of Analytical Methods in Chemistry, 2020 (2020) 6676320. https://doi.org/10.1155/2020/6676320

[25] A. Boumaza, A. Djelloul, F. Guerrab, Specific signatures of α-alumina powders prepared by calcination of boehmite or gibbsite, Powder Technol. 201 (2010) 177–180. https://doi.org/10.1016/j.powtec.2010.03.036

[26] K. Prem Ananth, S. Shanmugam, S.P. Jose, A.J. Nathanael, T.H. Oh, D. Mangalaraj, A.M. Ballamurugan, Structural and chemical analysis of silica-doped β-TCP ceramic coatings on surgical grade 316L SS for possible biomedical application, J. Asian Ceram. Soc. 3 (2015) 317–324. https://doi.org/10.1016/j.jascer.2015.06.004

[27] J. Buongiorno, et al. A benchmark study on the thermal conductivity of nanofluids, J. Appl. Phys. 106 (2009) 094312. https://doi.org/10.1063/1.3245330